HIGH-EFFICIENCY AMORPHOUS SILICON AND NANOCRYSTALLINE SILICON BASED SOLAR CELLS AND MODULES

Quarterly Technical Progress Report
May 1 through July 31, 2006

S. Guha and J. Yang
United Solar Ovonic LLC
Troy, Michigan

NREL Technical Monitor: Bolko von Roedern

Prepared under Subcontract No. ZXL-6-44205-14

Table of Contents

Preface

This Quarterly Report covers the work performed by United Solar Ovonic LLC under the Thin Film Partnership Subcontract No. ZXL-6-44205-14 for the period from May 1, 2006 to July 31, 2006. The following personnel participated in this research program.

A. Banerjee, E. Chen, G. Fischer, S. Guha (Principal Investigator), B. Hang, M. Hopson, A. Mohsin, J. Noch, J. M. Owens, T. Palmer, L. M. Sivec, D. Wolf, B. Yan, J. Yang (Co-Principal Investigator), K. Younan, and G. Yue.

Collaboration with the Colorado School of Mines, University of Oregon, Syracuse University, and National Renewable Energy Laboratory is acknowledged.

1. Large-area a-Si:H/a-SiGe:H/a-SiGe:H triple-junction cells made under the manufacturing constraints

1.1. Introduction

One of our major objectives of this project is to develop new deposition parameters for improving solar cell efficiency and throughput, and hence reducing the cost of manufacturing. The spectrum splitting a-Si:H/a-SiGe:H/a-SiGe:H triple-junction structure on Al/ZnO back reflector is used in our 25 MW manufacturing line. Therefore, one task of the project is to optimize the deposition parameters of a-Si:H/a-SiGe:H/a-SiGe:H triple-junction solar cells under the manufacturing constraints, mainly the deposition time of each layer. Previously, we have achieved a stable total-area (0.268 cm^2) cell efficiency of 9.1% and stable aperture-area (460 cm^2) module efficiency of 8.9% using our large-area batch machine. Those cells were deposited with a Si_2H_6 and GeH_4 mixture under the manufacturing constraints on Al/ZnO back reflectors (BR). In order to reduce the cost, we have switched to a SiH_4 and GeH_4 mixture in the manufacturing process. In the research and development department, we have also studied the optimization of the deposition condition using the SiH_4 and GeH_4 mixture and we achieved a stable total-area (0.268 cm^2) triple-junction cell efficiency of 9.1%, which is similar to the result obtained with the Si_2H_6 and GeH_4 mixture. This result proved that in principle one can achieve a similar performance using inexpensive SiH_4 instead of Si_2H_6 for cells deposited under manufacturing constraints In this quarter, we have carried out optimization of large-area deposition of a-Si:H/a-SiGe:H/a-SiGe:H triple-junction solar cells using a SiH_4 and GeH_4 gas mixture on Al/ZnO back reflectors obtained from the 25 MW machine.

1.2. Experimental

We used one of our large-area batch machines (2B) for the deposition of a-Si:H and a-SiGe:H intrinsic layers as well as the doped layers. The deposition time of each layer is fixed according to the calculation with the web speed and the chamber lengths of the production line. The optimization of cell performance and uniformity were carried out using small ITO dots with an active-area of 0.25 cm^2. Large-area (>400 cm^2) modules were made using the center area of the substrate with wires and bus-bars. The large-area modules were encapsulated with a procedure similar to that in the manufacturing process. The small-area cells were measured using an AM1.5 ORC solar simulator with quantum efficiency (QE) correction for the short-circuit current density. The large-area modules were measured at various states of light soaking using a Spire solar simulator with an NREL calibrated c-Si solar cell with a proper filter. The light soaking experiments were done under 100 mW/cm^2 white light at 50 °C for over 1000 hours.

1.3. Small area cell performance and uniformity

The uniformity of thickness and cell performance is a major concern for large-area deposition. In order to obtain high module efficiency, the cell performance has to satisfy certain uniformity requirements. We deposited the samples on a large-area (14×15 in^2) substrate and then cut them into 1.85×1.85 in^2 pieces at different locations. Since we normally make 8.5×8.5 in^2 modules, we cut nine such pieces from an area 9.2×9.2 in^2. One is in the center of the

Table I: J-V characteristics of a-Si:H/a-SiGe:H/a-SiGe:H triple-junction cells at different locations of a large-area deposition (2B 11147), where the J_{sc} was taken directly from the J-V measurements. QE current densities and QE corrected efficiency (Eff^Q) of five cells are listed as a reference.

Location in 2B 11147	J_{sc} (mA/cm^2)	V_{oc} (V)	FF	Eff (%)	Eff^Q (%)	QE (mA/cm^2)		
						Top	Mid.	Bot.
Left North	7.41	2.195	0.656	10.67				
Left Center	7.40	2.220	0.659	10.82				
Left South	7.27	2.238	0.663	10.78	10.62	7.28	7.16	7.36
Central North	7.18	2.238	0.688	11.06	10.92	7.09	7.20	7.22
Central Center	7.24	2.237	0.679	10.98	10.66	7.02	7.31	7.28
Central South	7.22	2.207	0.676	10.77	10.49	7.03	7.49	7.32
Right North	7.47	2.161	0.623	10.05				
Right Center	7.49	2.122	0.634	10.28	9.83	7.31	7.41	7.48
Right South	7.38	2.159	0.636	10.14				
Average	7.34	2.197	0.657	10.62				

substrate, four at the middle of each edge, and four at each corner of the 9.2×9.2 in^2 area. Sixteen small ITO dots, with an active-area of 0.25 cm^2, were deposited on the nine pieces for J-V and QE measurements. Table I lists the cell performance from one run (2B 11147). The J-V data for each location are averages of the measurements on four cells. The uniformity of the cell performance in the given area is reasonably good. The highest initial J-V measured active-area efficiency is 11.06% (QE corrected 10.92%), and the average is 10.62% with a non-uniformity of ±5%. This uniformity is acceptable for large-area modules.

1.4. Large area module

Several large-area modules have been made with the same deposition recipe as the cells shown in Table I (2B 11147). The modules were measured at the states before and after lamination as well as light soaked for different times. Table II lists the aperture-area performance of four modules. The data presented here are as-measured data without spectral mismatch corrections. The encapsulation causes a decrease of 1-4% in J_{sc}, 0.4-1.0% in V_{oc}, but an increase of 0-1.5% in FF. The major light-induced degradation appears in the first 500 hours. The change in the last 500 hours is very small. The average light-induced degradation is about 15.7%, which is similar to that observed in our previous experiments of a-Si:H/a-SiGe:H/a-SiGe:H triple-junction solar cells. The major change is in the FF, where an average of 10.6% reduction appears after light soaking. The best stable aperture-area efficiency is 8.6%, which is slightly lower than the best module efficiency of 8.9% achieved using a Si_2H_6 and GeH_4 mixture. Figure 1 shows the J-V characteristics of the best module in the three states.

It is well known that the efficiency measured under a given solar simulator with a calibrated reference cell is not necessarily the same as under the standard AM1.5 illumination due to the difference in their spectra. Normally two major errors appear in J_{sc} and FF. First is the difference in the spectrum of the light source and the ideal AM1.5 spectrum as well as the difference in the QE spectra of the testing and reference cells, both of which cause an error in J_{sc}. Second, the non-ideal AM1.5 spectrum of the light source causes a difference in the current

Table II: Summary of a-Si:H/a-SiGe:H/a-SiGe:H triple-junction module performance in different states. Eff^T(%) is temperature corrected efficiency at 25 °C.

Sample 2B#	State	Area (cm^2)	T (^oC)	I_{sc} (A)	J_{sc} (mA/cm^2)	V_{oc} (V)	FF	P_{max} (W)	Eff (%)	Eff^T(%)
10386	Before lamination	420.0	24.2	2.960	7.05	2.190	0.654	4.24	10.09	10.08
	After lamination	413.8	24.2	2.882	6.96	2.180	0.662	4.16	10.05	10.04
	Change due to lamination				-1.3%	-0.5%	1.2%			-0.4%
	585-hour light soaking	413.8	24.2	2.820	6.81	2.100	0.606	3.58	8.65	8.64
	1004-hour light soaking	413.8	25.1	2.813	6.80	2.090	0.599	3.52	8.51	8.51
	Change due to light soaking				-2.3%	-4.1%	-9.5%			-15.2%
10383	Before lamination	420.0	23.9	2.947	7.02	2.210	0.662	4.31	10.25	10.24
	After lamination	416.0	25.1	2.876	6.91	2.180	0.671	4.20	10.10	10.11
	Change due to lamination				-1.6%	-1.4%	1.3%			-1.3%
	585-hour light soaking	416.0	24.4	2.833	6.81	2.100	0.616	3.66	8.80	8.80
	1004-hour light soaking	416.0	24.9	2.811	6.76	2.100	0.609	3.59	8.63	8.63
	Change due to light soaking				-2.2%	-3.7%	-9.2%			-14.6%
11156	Before lamination	462.0	23.7	3.382	7.32	2.230	0.645	4.87	10.54	10.53
	After lamination	458.0	24.2	3.239	7.07	2.220	0.654	4.70	10.26	10.25
	Change due to lamination				-3.4%	-0.4%	1.4%	-3.5%	-2.6%	-2.7%
	585-hour light soaking	458.0	24.7	3.236	7.07	2.13	0.584	4.02	8.78	8.78
	1004-hour light soaking	458.0	24.9	3.231	7.05	2.12	0.569	3.89	8.50	8.50
	Change due to light soaking				-0.3%	-4.5%	-13.1%			-17.0%
11166	Before lamination	462.0	23.7	3.349	7.25	2.230	0.650	4.85	10.50	10.47
	After lamination	458.0	24.4	3.215	7.02	2.210	0.651	4.63	10.11	10.10
	Change due to lamination				-3.2%	-0.9%	0.2%	-4.5%	-3.7%	-3.5%
	585-hour light soaking	458.0	24.4	3.199	6.98	2.110	0.581	3.92	8.56	8.55
	1004-hour light soaking	458.0	25.4	3.176	6.93	2.110	0.578	3.88	8.47	8.47
	Change due to light soaking				-1.3%	-4.5%	-11.2%			-16.1%

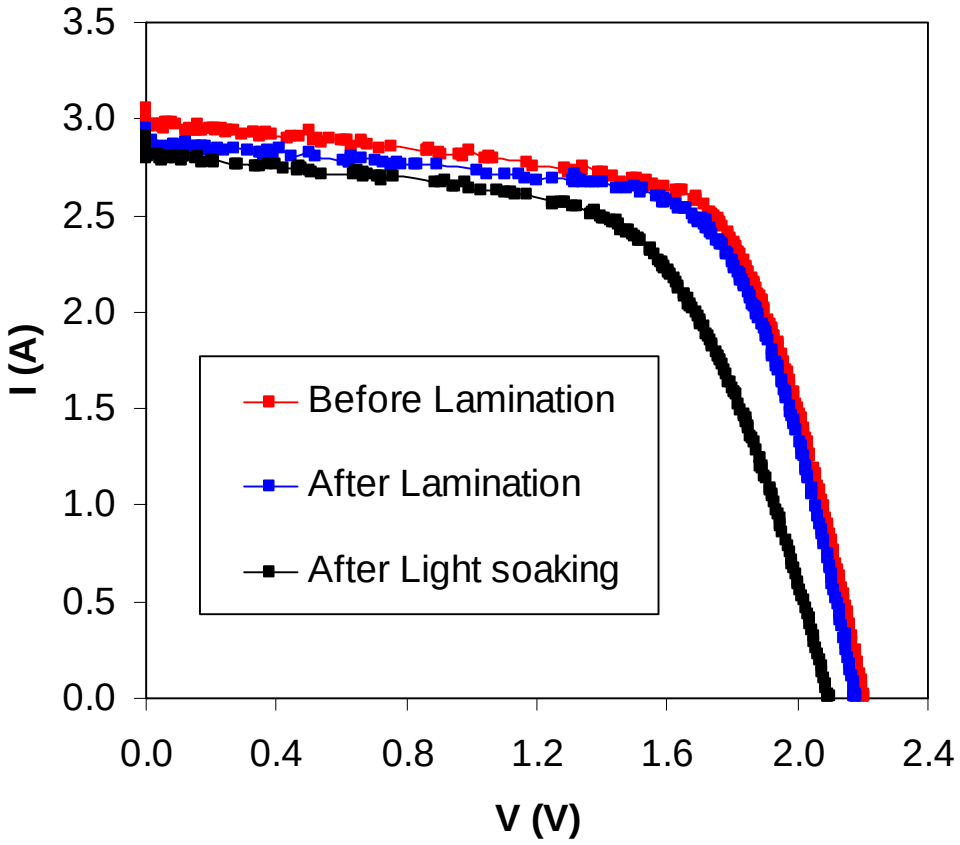

Figure 1. I-V characteristics of an a-Si:H/a-SiGe:H/a-SiGe:H triple-junction solar cell (2B 10383) before and after lamination, as well as after light soaking.

Table III: Summary of J-V characteristics of a-Si:H/a-SiGe:H/a-SiGe:H triple-junction solar cells at various states. The small area (1.2 cm^2) samples were taken from adjacent sections of the large area modules 2B 11156 and 11166 shown in Table II. B-Lam represents the state before lamination; L-Soak represents the state after lamination and light soaking.

Sample #	State	Eff (%)	J_{sc} (mA/cm^2)	V_{oc} (V)	FF	QE (mA/cm^2)		
						Top	Middle	Bottom
11156-3	B-Lam	9.85	6.77	2.168	0.671	6.77	7.30	7.01
	L-Soak	8.20	6.60	2.079	0.598	6.60	7.26	6.88
11156-5	B-Lam	10.12	6.97	2.177	0.667	6.97	7.39	7.23
	L-Soak	8.18	6.64	2.074	0.594	6.64	7.20	7.08
11166-1	B-Lam	10.34	6.90	2.226	0.673	7.01	6.90	6.99
	L-Soak	8.40	6.67	2.125	0.593	6.73	6.67	6.78
11166-3	B-Lam	10.34	6.93	2.230	0.669	6.97	6.93	7.07
	L-Soak	8.38	6.61	2.124	0.597	6.61	6.72	6.85

Table IV: The M factor of a-Si:H/a-SiGe:H/a-SiGe:H triple-junction solar cells in the states before and after lamination (Lam) as well as after light soaking (LS). The Uni-Solar Spire solar simulator spectrum was used.

Sample #	State	M Factor			
		Top	Middle	Bottom	Overall
11156-3	Before Lam	0.957	1.024	1.060	0.957
	After Lam	0.981	1.024	1.060	0.981
	After LS	0.980	1.023	1.060	**0.980**
11156-5	Before Lam	0.959	1.024	1.066	0.959
	After Lam	0.981	1.024	1.062	0.981
	After LS	0.981	1.023	1.022	**0.981**
11166-1	Before Lam	0.961	1.023	1.065	0.967
	After Lam	0.981	1.026	1.064	0.981
	After LS	0.981	1.024	1.065	**0.991**
11166-3	Before Lam	0.977	1.024	1.064	0.977
	After Lam	0.981	1.025	1.065	0.981
	After LS	0.981	1.024	1.065	**0.981**

mismatching of the component cells, which results in an error in FF.

In principle, the error in the J_{sc} of a single-junction solar cell can be corrected by adjusting the light intensity of the solar simulator based on an M factor calculated by,

$$M = \frac{\int E_R(\lambda)Q_R(\lambda)d\lambda \times \int E_S(\lambda)Q_T(\lambda)d\lambda}{\int E_S(\lambda)Q_R(\lambda)d\lambda \times \int E_R(\lambda)Q_T(\lambda)d\lambda},$$

where $E_R(\lambda)$ is the reference light source (AM1.5) spectrum, $E_S(\lambda)$ the test light source (solar simulator) spectrum, $Q_R(\lambda)$ the quantum efficiency of reference cell, and $Q_T(\lambda)$ the Quantum efficiency of test cell. For a multi-junction cell, the M factor becomes,

$$M = \frac{\int E_R(\lambda)Q_R(\lambda)d\lambda \times \int E_S(\lambda)Q_T(i,\lambda)d\lambda}{\int E_S(\lambda)Q_R(\lambda)d\lambda \times \int E_R(\lambda)Q_T(j,\lambda)d\lambda},$$

where *i* and *j* represent the limiting cells under the test light source and the reference light source, respectively. In order to obtain a corrected J_{sc}, one can reduce the test light intensity by a factor of 1/M, or use the measured J_{sc} under the standard setting condition and divide it by the M factor.

Theoretically, the M-factor correction can provide a more accurate measurement of J_{sc}. However, practically, more errors could be introduced by the errors in the QE of the testing cell. The major problem is that it is hard to measure the QE of large-area modules. An alternative way is to use the QE measured from a different cell with a small area but made under the same condition. In most cases, one uses QE data from a small-area cell without encapsulation. It is well known that the encapsulation changes the QE curves, and therefore, the M factor.

In this study, we tried to make the measurement more accurate by using QE data that are close to the QE of real modules. We used adjacent pieces from the module fabrication and made small-area (1.2 cm^2) cells with the same wires and bus-bars as used in the module fabrication. We also encapsulated the small-area cells and light soaked them using the same procedures as the large-area modules. The QE were measured at different states for calculating the M factor. Table III lists the J-V characteristics and QE current densities of four small-area cells from two

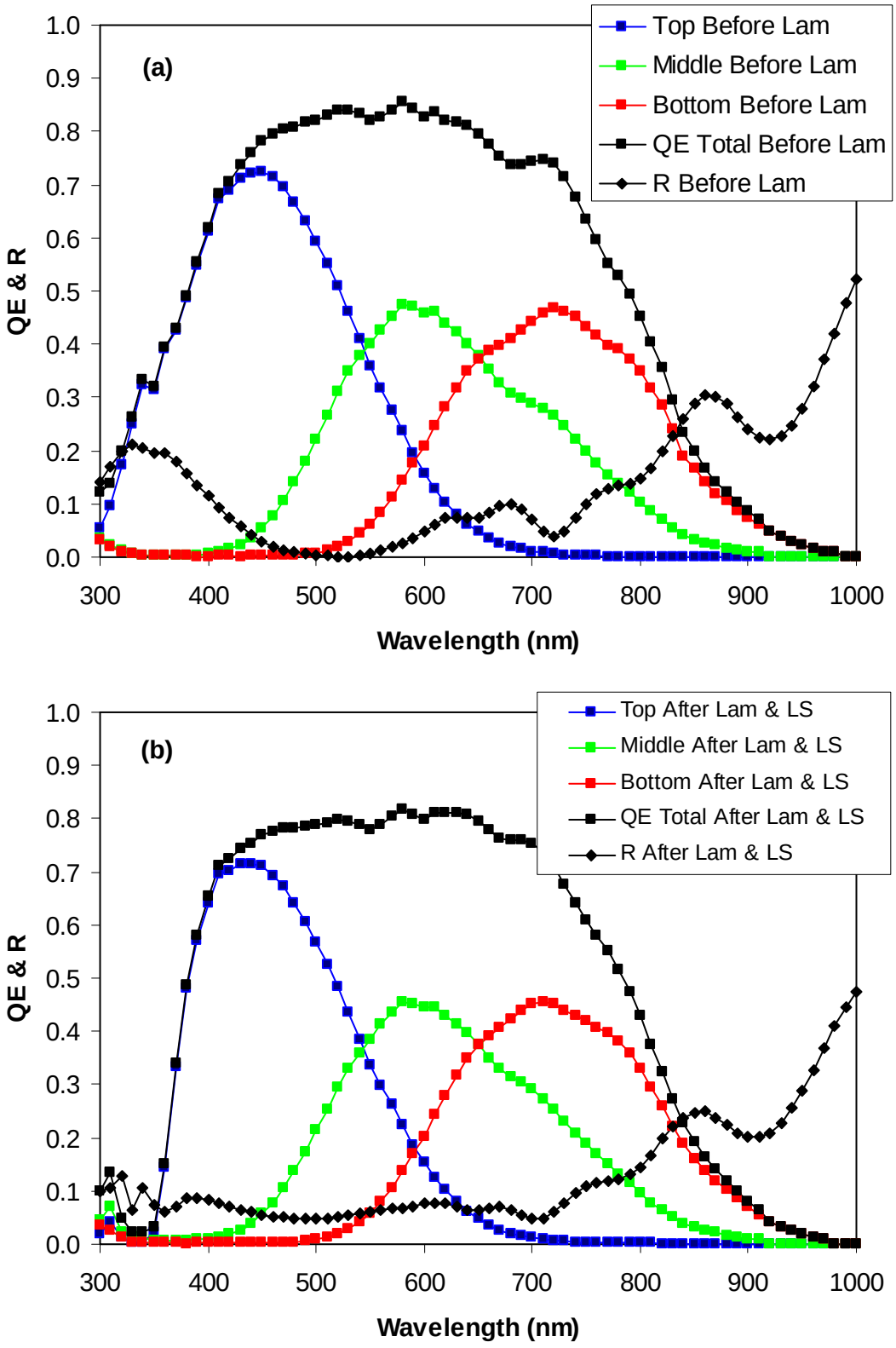

Figure 2. Quantum efficiency (QE) and reflection (R) curves of an a-Si:H/a-SiGe:H/a-SiGe:H triple-junction cell on Al/ZnO (a) before lamination and (b) after lamination and light soaking.

large-area depositions that were used for module fabrication. It appears that the small-area cells have a slightly smaller V_{oc} and J_{sc}, but a slightly larger FF than the large-area modules at each corresponding state, which could be due to the non-uniformity of the deposition. Figure 2 gives an example of the QE changes from the initial non-encapsulated state to the encapsulated and light-soaked state. Corresponding reflection curves are also presented. The QE curves change dramatically at the short wavelength below 400 nm. We calculated the M-factors of the four cells at the initial non-encapsulated state and the encapsulated and light soaked state using the measured QE data and the QE of our reference cell as well as the spectrum of our Spire solar simulator. Table IV summarizes the M-factors of four cells at the two states. On average, the M factor is about 0.965 in the initial non-encapsulated state, and 0.983 in the final encapsulated and light-soaked state. If we take the M factor into account, the highest stable encapsulated module efficiency should be 8.78%. We shall send these modules to NREL for measurement.

1.5. Summary

We have optimized large-area deposition of a-Si:H/a-SiGe:H/a-SiGe:H triple-junction solar cells under the manufacturing constraints with a SiH_4 and GeH_4 gas mixture on Al/ZnO back reflectors from the manufacturing line. A stable aperture-area (416 cm^2) efficiency of 8.6% has been achieved. With the spectrum mismatching correction, this efficiency could be 8.8%, which is similar to the highest module efficiency previously achieved using a Si_2H_6 and GeH_4 gas mixture.

2. High rate deposition of a-Si:H solar cells using modified very high frequency glow discharge

2.1. Introduction

A high deposition rate for making solar cell intrinsic layers is always desirable to enhance the throughput and reduce the production cost. However, a-Si:H solar cells made with the conventional radio frequency (RF) glow discharge at high rates exhibit poor quality. The materials contain a high defect density, microvoids, and di-hydride structures, which lead to a low initial efficiency and poor stability in solar cells. In our current manufacture machine the deposition rate is about 3 Å/s. New deposition techniques are needed to increase the deposition rate without compromising the material quality. Obviously, increasing the deposition rate will directly increase the annual capacity or reduce the initial capital investment on the machine.

Very high frequency (VHF) glow discharge has been widely used in the deposition of a-Si:H and nc-Si:H materials and devices. Compared to the conventional RF technique, VHF plasma has higher electron density and lower ion energy, which is believed to increase the deposition rate and improve the material quality. In our laboratory, we have used a modified VHF (MVHF) system to make a-Si:H, a-SiGe:H, and nc-Si:H solar cells. An initial efficiency of 11.2% was obtained in an a-Si:H/a-SiGe:H double-junction solar cell with the top cell intrinsic layer deposited at 8 Å/s and the bottom cell at 6 Å/s. Recently, we have achieved an initial active-area efficiency of 9.0% with a nc-Si:H single-junction solar cell and a stabilized active efficiency of 13.3% with an a-Si:H/nc-Si:H/nc-Si:H triple junction solar cell. In this quarter, we have optimized the deposition condition of a-Si:H in a wider growth parameter space, mainly in the higher pressure and smaller gap spacing regime. We have systematically studied the initial cell performance and stability as a function of the deposition rate.

2.2. Initial performance of a-Si:H solar cells made with MVHF at high deposition rates

A series of a-Si:H *n-i-p* solar cells has been made with an MVHF high rate a-Si:H intrinsic layer and low rate RF doped layers. Under each deposition condition, two runs were made: one on a specular stainless steel (SS) substrate and one on a Ag/ZnO back reflector (BR) coated SS substrate. The deposition rate of the a-Si:H intrinsic layer was changed from 5 to 14 Å/s by varying the VHF power and the pressure. The thickness of the intrinsic layer was controlled in the range of 200-220 nm. ITO dots with an active-area of 0.25 cm^2 were deposited on the *p* layer for J-V and QE measurements.

The deposition rate of a-Si:H depends on many deposition parameters such as the excitation (VHF or RF) power, gas pressure, and gas dilution ratio. Under a given condition, the most common way to increase the deposition rate is to increase the excitation power. Figure 3 shows the deposition rate of a-Si:H as a function of VHF power. One can see that the deposition rate continues to increase with the VHF power in the range of 9-14 Å/s. The deposition rate is also very sensitive to the gas pressure. In the high pressure regime, increasing the pressure leads to a decrease in the deposition rate. In this study, we focused on the range of deposition rate from 5 to 14 Å/s.

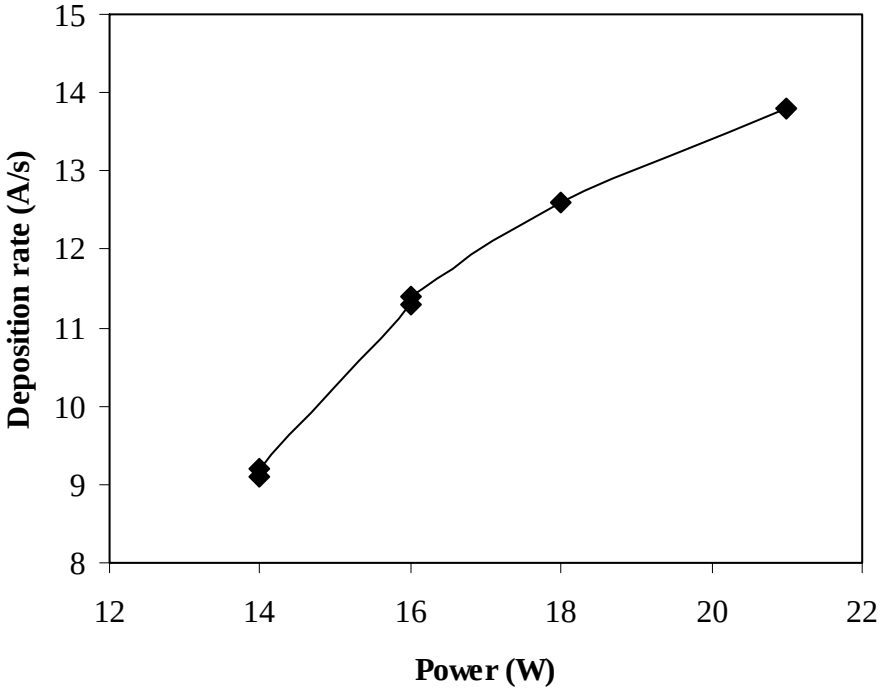

Figure 3. The deposition rate of a-Si:H as a function of VHF power.

Table V: Performance of a-Si:H solar cells made with MVHF on BR and SS substrates. FFB_{bB} and FFB_{rB} represent the FF measured under weak blue and red lights, respectively. The values of JB_{scB} are from QE calibration.

Sample No.	VB_{ocB} (V)	FF	FFB_{bB}	FFB_{rB}	JB_{sc} (mA/cmP^{2P})	Eff (%)	Substrate	Rate (Å/s)	*i* layer time (seconds)
14325	0.983	0.712	0.759	0.753	14.34	10.04	BR	5.2	420
14166	1.000	0.735	0.767	0.749	9.71	7.14	SS		
14324	1.001	0.723	0.763	0.750	13.68	9.90	BR	6.1	300
14139	0.974	0.727	0.765	0.780	9.62	6.81	SS		
14347	0.987	0.702	0.722	0.744	14.67	10.16	BR	9.2	288
14336	0.988	0.710	0.760	0.770	10.36	7.27	SS		
14323	0.993	0.709	0.741	0.741	14.69	10.34	BR	9.3	240
14318	0.978	0.697	0.754	0.763	10.48	7.14	SS		
14346	0.986	0.696	0.716	0.742	14.46	9.92	BR	11.4	222
14335	0.995	0.698	0.764	0.747	10.43	7.24	SS		
14338	0.997	0.704	0.743	0.751	13.68	9.60	BR	11.9	180
14330	0.985	0.714	0.755	0.768	9.96	7.00	SS		
14345	0.984	0.697	0.717	0.742	14.20	9.74	BR	12.6	175
14342	0.986	0.713	0.760	0.767	9.89	6.95	SS		
14348	0.982	0.710	0.717	0.743	14.11	9.84	BR	13.8	156
14333	0.995	0.713	0.769	0.763	9.64	6.84	SS		

Table V lists the J-V characteristics of the cells on both SS and BR substrates, where the data of J_{sc} are from the integrals of the QE and AM1.5 solar spectrum. FF_b and FF_r denote the FF obtained from the measurements with weak blue and red lights, respectively. Normally, we believe that the FF_b probes the interface between the *i* and *p* layers, while the FF_r detects the quality of the *i* layer. One can see that the cell performance does not have a strong dependence on the deposition rate. Most cells show a high FF_r, indicating a high quality of the a-Si:H intrinsic layer. The average efficiency is around 7% for the cells on SS and 10% on BR. Compared to the cells on SS, the V_{oc} and FF do not change much for the cells on BR, but the J_{sc} is increased by 40 % due to light trapping, which directly improves the cell efficiency. The intrinsic layer thickness was controlled in the range of 200-220 nm for each sample. By increasing the intrinsic layer thickness to 330 nm, an efficiency of 10.6% (J_{sc}=15.94 mA/cm^2, V_{oc}=0.993 V, and FF=0.674) has been obtained with an a-Si:H single-junction cell on BR deposited at 10 Å/s.

Table VI. Stability results of a-Si:H solar cells on Ag/ZnO BR coated SS made by VHF at high rates. For comparison, a sample (14028) made by RF at a low rate of 1.0 Å/s has been light-soaked together. The thickness for all samples is in the range of 200-220 nm.

Sample No.	State	VB_{ocB} (V)	FF			JB_{sc} (mA/cmP^2 $_P$)	Eff (%)	Rate (Å/s)
			AM1.5	FFB_{bB}	FFB_{rB}			
14028	Initial	1.020	0.695	0.740	0.719	13.78	9.77	1.0
	Stable	0.998	0.640	0.636	0.653	13.12	8.38	
	Deg(%)	2.2%	7.9%			4.8%	14.2%	
14325	Initial	0.983	0.712	0.759	0.753	14.34	10.04	5.2
	Stable	0.951	0.645	0.677	0.665	13.92	8.54	
	Deg(%)	3.3%	9.4%			2.9%	14.9%	
14324	Initial	1.001	0.723	0.763	0.750	13.68	9.90	6.1
	Stable	0.965	0.668	0.697	0.676	13.05	8.41	
	Deg(%)	3.6%	7.6%			4.6%	15.1%	
14347	Initial	0.987	0.702	0.722	0.744	14.67	10.16	9.2
	Stable	0.958	0.645	0.647	0.667	13.67	8.45	
	Deg(%)	2.9%	8.1%			6.8%	16.8%	
14323	Initial	0.993	0.709	0.741	0.741	14.69	10.34	9.3
	Stable	0.956	0.649	0.644	0.639	13.92	8.64	
	Deg(%)	3.7%	8.5%			5.2%	16.4%	
14346	Initial	0.986	0.696	0.716	0.742	14.46	9.92	11.4
	Stable	0.960	0.655	0.663	0.684	13.49	8.48	
	Deg(%)	2.6%	5.9%			7.2%	14.5%	
14338	Initial	0.997	0.704	0.743	0.751	13.68	9.60	11.9
	Stable	0.959	0.645	0.681	0.672	13.20	8.15	
	Deg(%)	3.8%	8.4%			3.5%	15.1%	
14345	Initial	0.984	0.697	0.717	0.742	14.20	9.74	12.6
	Stable	0.960	0.648	0.656	0.675	13.41	8.34	
	Deg(%)	2.4%	7.0%			5.6%	14.4%	
14348	Initial	0.982	0.710	0.717	0.743	14.11	9.84	13.8
	Stable	0.959	0.659	0.662	0.673	13.34	8.43	
	Deg(%)	2.3%	7.2%			5.5%	14.3%	

Table VII: Stability results of MVHF high rate a-Si:H solar cells on SS. As a reference, a RF low rate a-Si:H cell RF (13899) is also included. The thicknesses for all samples are in the range of 200-220 nm.

Sample No.	State	VB_{ocB} (V)	FF			JB_{sc} (mA/cmP^2_P)	Eff (%)	Rate (Å/s)
			AM1.5	Blue	Red			
13899	Initial	1.014	0.748	0.782	0.760	9.82	7.45	1.0
	Stable	0.974	0.676	0.720	0.677	9.37	6.17	
	Deg. (%)	3.94%	9.63%			4.58%	17.2%	
14166	Initial	1.002	0.732	0.775	0.760	9.71	7.14	5.2
	Stable	0.959	0.661	0.697	0.655	9.41	5.96	
	Deg. (%)	4.3%	9.7%			3.1%	16.5%	
14308	Initial	0.997	0.733	0.782	0.751	9.61	7.07	7.5
	Stable	0.958	0.663	0.721	0.669	9.30	5.91	
	Deg. (%)	3.9%	9.5%			3.2%	16.4%	
14309	Initial	0.979	0.699	0.776	0.752	10.09	6.94	9.0
	Stable	0.944	0.636	0.702	0.636	9.71	5.83	
	Deg. (%)	3.6%	9.0%			3.8%	16.0%	
14318	Initial	0.979	0.702	0.757	0.762	10.48	7.14	9.3
	Stable	0.943	0.626	0.688	0.648	10.05	5.93	
	Deg. (%)	3.7%	10.8%			4.1%	16.9%	
14370	Initial	0.984	0.713	0.756	0.769	10.14	7.11	11.3
	Stable	0.950	0.673	0.687	0.666	9.45	6.04	
	Deg. (%)	3.5%	5.6%			6.8%	15.0%	
14342	Initial	0.986	0.713	0.762	0.765	9.89	6.95	12.6
	Stable	0.952	0.647	0.678	0.670	9.33	5.75	
	Deg. (%)	3.2%	9.3%			5.7%	17.3%	
14333	Initial	0.995	0.713	0.760	0.754	9.64	6.84	13.8
	Stable	0.957	0.650	0.694	0.653	9.17	5.70	
	Deg. (%)	3.8%	8.8%			4.9%	16.7%	

2.3. Stability of a-Si:H solar cells made with MVHF at different deposition rates

Stability testing has been done for all the cells with different deposition rates on SS and BR. The solar cells were light soaked under 100 mW/cm^2 white light at 50 ^oC for 1000 hours. As a reference, two a-Si:H cells made with RF at a low rate ~1.0 Å/s (one on SS and one on Ag/ZnO BR) were light-soaked together with the high rate MVHF cells. The results are listed in Tables VI and VII for the cells on BR and on SS, respectively. Figure 4 shows the initial and stable efficiencies as well as the light-induced degradation as a function of the deposition rate. The light-induced degradation rate of the efficiency varies from 15% to 17% for cells on both BR and SS, but it does not show any dependence on the deposition rate. The highest stabilized efficiency of 8.64% has been achieved with an a-Si:H single-junction cell made at 9.3 Å/s on BR

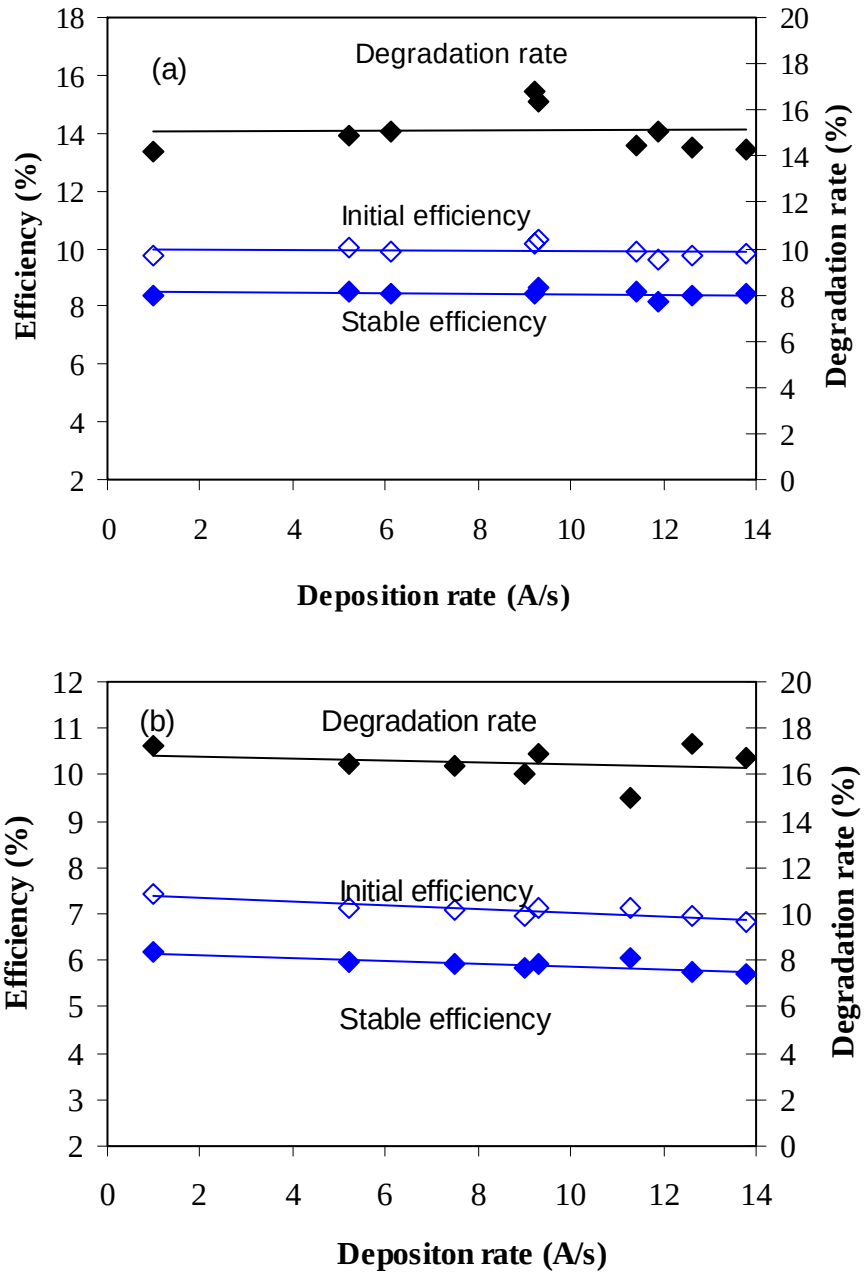

Figure 4. The efficiency before and after light-soaking, and the degradation rate as a function of deposition rate for the cells on (a) BR and (b) SS.

.

2.4. Summary

In summary, we have found that the MVHF-deposited a-Si:H solar cells showed good initial efficiency and stability. The most important result is that the cell performance and stability do not depend on the deposition rate up to 14 Å/s. This phenomenon is quite different from the cells made using RF at high rates. The degradation rate of the RF-cells usually increases with the deposition rate.